Deformation micromechanics: Deformation micromechanics studies were carried out using simultaneous Raman spectroscopy and either tensile or 4-point bending tests. For tensile deformation, an Instron 1122 testing machine was used simultaneously with the remote Raman Renishaw system 100. The 4-point bending tests were carried out according to the ASTM standard using a rig attached to the stage of the optical microscope of a Renishaw system 1000. The 632.8 nm red line of He-Ne laser was used in both the Renishaw 100 and 1000 systems. In all cases, the strains in coatings were measured independently using Series EA strain gauges with 6 mm gauge length and with a nominal resistance value of 120 Ω (Measurements Group Inc.).

[1] P. Colomban, J. Corset, *J. Raman Spectroscopy* **1999**, *30*, 863.
[2] B. Dietrich, K. F. Dombrowski, *J. Raman Spectroscopy* **1999**, *30*, 893.
[3] H. Miyagawa, D. Kamiya, C. Sato, et al., *J. Mater. Sci.* **1999**, *34*, 105.
[4] B. D. Batchelder D. N., *J. Polymer Sci., Polymer Physics Ed.* **1979**, *17*, 569.
[5] A. J. Campbell, C. K. L. Davies, D. N. Batchelder, *Macromol. Chem. Phys.* **1998**, *199*, 109.
[6] J. L. Stanford, R. J. Day, X. Hu, et al., *Progr. Organic Coat.* **1992**, *20*, 425.
[7] X. Hu, J. L. Stanford, R. J. Day, et al., *Macromol.* **1992**, *25*, 684.
[8] X. Hu, R. J. Day, J. L. Stanford, et al., *J. Mater. Sci.* **1992**, *27*, 5958.
[9] X. Hu, J. L. Stanford, R. J. Young, *Polymer* **1994**, *35*, 80.
[10] C. A. Cooper , R. J. Young, *J. Raman Spectroscopy* **1999**, *30*, 929.
[11] C. A. Cooper, R. J. Young, M. Halsall, *Composites Part A* **2001**, *32*, 401.
[12] Z. Jia, Z. Wang, C. Xu, et al., *Mater. Sci. Eng. A* **1999**, *271*, 395.
[13] J. R. Wood, Q. Zhao, M. D. Frogley, et al., *Phys. Rev. B* **2000**, *62*, 7571.
[14] J. R. Wood, Q. Zhao, H. D. Wagner, *Composites Part A* **2001**, *32*, 391.
[15] Q. Zhao, M. D. Frogley, H. D. Wagner, *Composites Sci. Technol.* **2002**, *62*, 147.
[16] M. S. Dresselhaus, G. Dresselhaus, A. Jorio, et al., *Carbon* **2002**, *40*, 2043.
[17] M. D. Frogley, Q. Zhao, H. D. Wagner, *Phys. Rev. B* **2002**, *65*, 113413.
[18] G. S. Duesberg, I. Loa, M. Burghard, et al., *Phys. Rev. Lett.* **2000**, *85*, 5436.

Processing of Transparent Conducting Coatings Made With Redispersible Crystalline Nanoparticles

By *Joerg Puetz,* *Naji Al-Dahoudi*, and *Michel A. Aegerter*

Recent developments in display and smart window technology depend fundamentally on transparent electrodes, both for electrical control and antistatic purposes. The required combination of an electrical conductivity with a high transmission in the visible range is found in a class of materials that is referred to as "transparent conducting oxides" (TCO) with ITO (In_2O_3:Sn), FTO (SnO_2:F), ATO (SnO_2:Sb) and (AZO) ZnO:Al being the most frequently used.[1] All these oxides are n-type doped wide band gap (> 3 eV) semiconductors in which doping is accomplished by exchange of oxygen (oxygen vacancies, F⁻) or replacement of a metal ion with an ion of higher oxidation state (e.g. Sn^{IV} in In_2O_3).

TCOs are always applied as thin films with a thickness much below 1 μm to keep the transmission high. The method of choice for display applications is magnetron sputtering as it gives the lowest resistivity with the best optical quality for ITO and AZO, but for architectural applications chemical vapor deposition (CVD) or spray pyrolysis of FTO are favored because of the much lower deposition cost.[2] All these processes require elevated temperatures of at least 200 °C (sputtering) to 500 °C (spray pyrolysis), so that coatings can only be deposited on glass substrates. The increasing demand for portable consumer electronics, however, is calling for a change for the lighter plastic films as substrates, but with a similar or only slightly decreased electrical conductivity.

There are currently two competing approaches aiming at the deposition of TCO coatings on plastics. One is based on the modification of magnetron sputtering for a semi-continuous deposition on plastic webs,[3] but the technical expenses still make the coatings too expensive for most applications and the electrical properties are often insufficient. Alternatively to these vacuum deposition techniques, wet coating techniques have already proven their suitably for web coating in industrial processes like for photographic films or the surface modification of papers.[4] The sol-gel process that is well-known for oxide coatings, however, cannot be used for plastics as high temperatures are required to obtain conducting films.[5]

[*] Dr. J. Puetz, Dr. N. Al-Dahoudi, Prof. M. A. Aegerter
Leibniz-Institut für Neue Materialien – INM
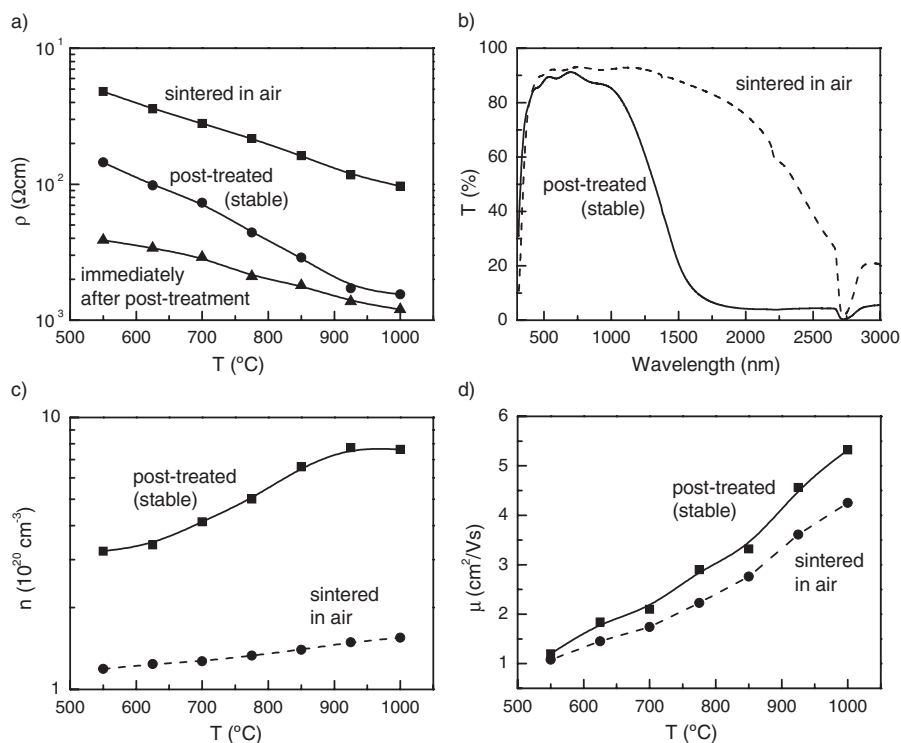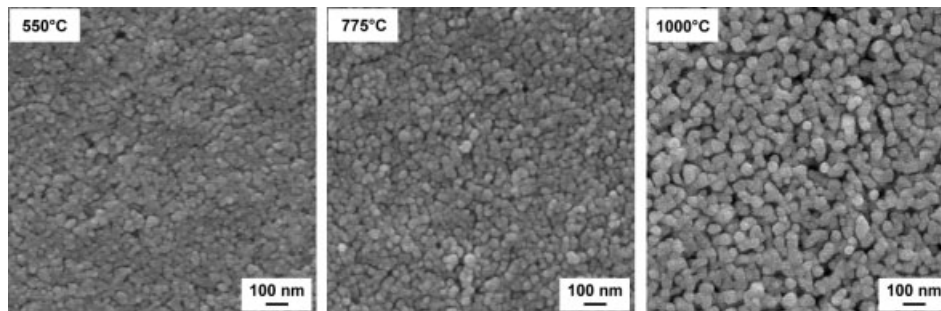Saarbruecken, Germany
E-mail: puetz@inm-gmbh.de

Fig. 2. SEM morphology of pure ITO nanoparticle films after sintering at temperatures of 550 °C, 775 °C and 1000 °C, respectively.

Ar) at 130 °C during 2 h further reduces the sheet resistance of the coatings.

The structural properties of the coatings were investigated using profilometry for the film thickness (P10, Tencor) and both scanning electron microscopy (SEM - JSM 6400F, JEOL; 10 kV) and cross-sectional high resolution transmission electron microscopy (HRTEM - CM200 FEG, Philips; 200 keV) for the surface and bulk morphology, respectively. Surface images of ITO patterns on larger scale were taken by a white light interferometer (WLI - Newview 5000, Zygo). The electrical properties were measured using a four-point probe and a combined van der Pauw/Hall measurement (MMR Technologies). Optical transmission spectra were collected for coatings on fused silica substrates against air reference (CARY 5E, Varian). The mechanical properties were determined according to standard test methods in terms of the adhesion (tape test - DIN 58196-K2; cross cut test - ASTM 3359 / DIN 53151), the abrasion resistance (cotton cloth and hard rubber DIN 58196-H25/G10; taber test - DIN 52347/CS10F/ 5.4 N) and the hardness (pencil test - ASTM 3363–92a).

Results and Discussion

High temperature processing: Transparent conducting ITO coatings can be prepared readily from dispersions of surface modified ITO nanoparticles by wet deposition followed by a conventional thermal treatment as in sol-gel processing. Due to the higher solid content and the lower shrinkage of the crystalline nanoparticles the resulting coatings have a significantly higher thickness of approx. 570 nm with a high transmission in the visible range (Fig. 1b, dashed line). But the corresponding electrical properties (Fig. 1a) with a resistivity of 5×10^{-2} Ωcm (corresponding to a sheet resistance of 1.2 k$\Omega_{\square}$) after sintering at 550 °C in air are not yet satisfying and at lower processing temperatures the sheet resistance is even in the order of several MΩ.

An improvement of the conductivity can be achieved by a post-treatment under reducing conditions with a minimum at 4×10^{-3} Ωcm after annealing in forming gas (350 °C, 30 min). This value is, however, not stable under ambient conditions in air and finally reaches 1.5×10^{-2} Ωcm after several days, which nevertheless is lower than the original value. The mechanism behind this reversible process is not yet understood, but it is certainly connected to the formation of oxy-

gen vacancies. Though the ITO nanoparticles were already treated in forming gas atmosphere during the synthesis, it is likely that a fraction of the oxygen vacancies especially at the particle surface gets lost during the wet processing and the high temperature treatment in air. These oxygen vacancies can be recovered in a post-treatment step under inert or reducing atmosphere but under exposure to oxygen the number of charge carriers is decreased again at the particle surface resulting in an increased resistivity. As the latter process usually takes place at room temperature it affects the number of charge carriers only superficially and hence the observed resistivity is still lower than after annealing in air. This model is supported by Hall measurements (Figs. 1c and 1d) which clearly show that the decreased resistivity after forming gas treatment is largely due to the higher density of charge carriers rather than to their mobility.

With increasing sintering temperature, the resistivity is lowered by a factor 4 to a value of 1.2×10^{-2} Ωcm at 1000 °C (Fig. 1a) coming along with a particle growth from 25 to 33 nm.[10] The post-treatment again leads to a significant decrease in the resistivity, but here the value after equilibration in air is much closer to the minimum value measured immediately after post-treatment. This becomes plausible if we consider that the interacting surface area is smaller for the larger, sintered particles and hence the influence on the total number of charge carriers is lower. The Hall measurements reveal that in fact the charge carrier density is responsible for this approximation of the values. But also the mobility of the
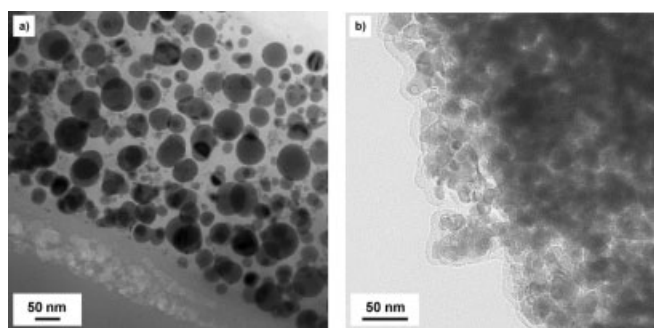

Fig. 3. HRTEM images of ITO/MPTS composites after a) heat treated at 130 °C and b) UV curing.
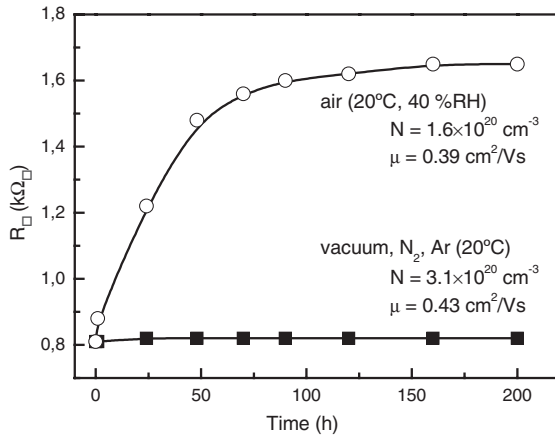
Fig. 4. Evolution of the sheet resistance of post-treated ITO/MPTS nanocomposite coatings during storage in air or under inert conditions (vacuum, N₂, Ar), respectively. The thickness of the coatings is approx. 570 nm.

charge carriers is slightly higher which can be interpreted in terms of larger crystallites and better interconnections between them.

As a result of the close relationship between the electrical and optical properties, the electronic changes during the post-treatment also show in the optical spectra (Fig. 1b). The forming gas treatment leads to a significant decrease of the transmission above 800 nm, which can only to a certain extent be explained by the increased density of charge carriers and the corresponding shift of the plasma edge. Instead, an additional absorption of the ITO in the near IR (800 nm to 2.5 μm) is clearly seen in the absorption spectra[10] possibly connected to defects in the material due to the oxygen deficiency.

The particle growth and the coalescence with increasing sintering temperature can be clearly observed in the SEM images as shown in Figure 2. The coatings still exhibit a granular structure with a high porosity explaining the significantly higher resistivity of these films compared to sputtered films (typically 1×10^{-4} Ωcm). The reason for this porosity is basically found in the spherical shape of the particles but also the surface modification and the organic solvents certainly impede a closer approach of the particles during film drying.

The loose structure with only isolated sintering necks already suggest poor mechanical properties of such coatings and in fact they can be wiped off even after sintering at 1000 °C (cloth test: class 2, tape test: passed[10]). A paramount task consequently is aiming on an improvement of the mechanical properties and the density to decrease the resistivity.

Low temperature UV processing: In order to improve the cohesion between the ITO nanoparticles, a chemical binder based on an organically modified silane was added to the ITO coating dispersion. Such organically modified silanes offer highest flexibility for film processing and curing due to their hybridic nature.[11] By a pre-hydrolysis an inorganic silicate-like network can be formed with a high mechanical strength and the possibility to bind to the inorganic ITO surface chemically. The choice of an organic side chain with special chemical functionalities, however, makes new curing methods possible as it has been realized using a double bond containing 3-methacryloxypropyl-trimethoxsilane (MPTS). In the presence of a photo initiator such coating systems now can be UV cured by radical polymerization at low temperature.

The role of the UV illumination for the morphology in the curing process of such ITO/MPTS nanocomposites has been investigated using electron microscopy (Fig. 3). With a moderate heating at 130 °C without UV light, the resulting coatings exhibit a dense surface structure but the cross-sectional HRTEM image (Fig. 3a) shows isolated ITO particles embedded in an amorphous matrix. This morphology very much resembles an emulsion like structure with agglomerates of the smaller ITO nanoparticles. Accordingly, the electrical conductivity of these samples is poor with a sheet resistance of several MΩ.

In contrast, the UV cured samples (approx. 10 J/cm²) shown in Figure 3b, exhibit a granular but cohesive structure with the ITO nanoparticles in direct contact and in their original particle size, i.e., without agglomeration. This structure allows a continuous conduction which shows in the much lower sheet resistance of the UV cured sample of only 8 kΩ. These results indicate that it is rather the polymerization of the double bond that is beneficial for the conductivity than the contribution of the pre-hydrolysed MPTS binder itself.

A sheet resistivity of 8 kΩ obtained after UV curing in air corresponds to a resistivity of 0.4 Ωcm for a 570 nm thick coating which is still at least three orders of magnitude higher than the best values obtained for sputtered coatings. But like in the case of the pure ITO films, a further decrease again can be achieved by a reducing post-treatment at low temperatures (up to 130 °C). Figure 4 shows the temporal evolution of the sheet resistance of such ITO/MPTS nanocomposite coatings after a forming gas treatment. While the sheet resistance
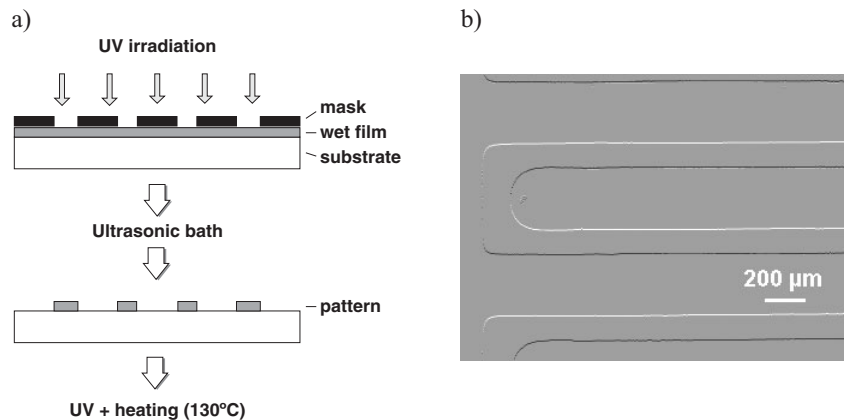
a)

b)

Fig. 5. Mask illumination procedure for wet films (a) and obtained ITO pattern on a PC substrate (b).

is stable under inert storing conditions (vacuum, N_2, Ar), it slowly increases by a factor of 2 reaching a constant value of 1.6 $k\Omega_\square$ after more than 150 h. It is most probably the same mechanism of oxygen adsorption and the loss of charge carriers that is responsible for this increase in sheet resistance. Compared to the pure ITO films, however, the process is rather slow as the density is higher and thus the diffusion of oxygen should be hindered. A closer investigation is confirming this assumption revealing that the increase is mainly caused by a drop in the charge carrier density from 3.1 to 1.6×10^{20} cm^{-3} whereas the mobility remains almost constant (0.39 and 0.43 cm^2/Vs, resp.).

The optical properties of the UV cured composite coatings in the visible range are similar to those of pure ITO (Fig. 1b) with a transmission larger than 85 % in the visible. Despite of the low content of the binder, the mechanical properties of the respective coatings could be improved significantly compared to the pure inorganic material. The coatings pass both the tape and the cross cut test, certifying a good adhesion even on plastic substrates. A testing of the abrasion resistance revealed no scratches after 10 rubbing cycles or after 25 rubbing cycles with the milder cotton cloth (both class 1). The results of the taber test with a haze of 15 % after 10 cycles, however, indicate that the coatings are still rather soft, which is confirmed by a hardness of 1 H determined by the pencil test. Superior mechanical properties could of course be obtained by an increased binder content, but this inevitably increases the resistivity of the coatings, so that in practice always a compromise has to be found between the electrical and mechanical properties of such TCO nanocomposite coatings.

UV patterning: The UV curing of ITO/MPTS nanocomposites cannot only be used to cure coatings but it can also be of advantage in the production of transparent conducting patterns, for example, for conductor lines or sensors. A common patterning method is found in the mask illumination process (Fig. 5a) in which the ITO film is covered with an impervious mask and is then exposed to UV light. In the exposed areas, the MPTS polymerizes and becomes insoluble in most solvents while the wet unexposed part of the film can easily be removed with ethanol in an ultrasonic bath. The remaining pattern is then again UV cured and heated to 130 °C to complete the polymerization and evaporate the solvents. Typical line widths that can be realized with this method are of the order of several tens of microns (Fig. 5b). Finer structures can be obtained by a direct laser writing process (e.g. at 350 nm) where the line width is basically determined by the diameter and the shape of the laser beam.[12]

Conclusions: Redispersible nanoparticles of transparent conducting ITO can be prepared reproducibly and in adequate amounts for industrial applications by a wet chemical processing. Dispersions obtained from such powders are characterized by a marked long-term stability and can be used in any kind of wet coating or printing technique to obtain transparent conducting coatings. Pure coatings of ITO nanoparticles, however, exhibit insufficient mechanical properties even after sintering at 1000 °C as the cohesion between the particles is still poor. It is therefore necessary to add a chemical binder like MPTS which both increases the load capacity and offers possibilities of a low-temperature processing. This way, transparent conducting coatings of an ITO nanocomposite with a thickness of up to 1 μm and a sheet resistance of 1 to 2 $k\Omega_\square$ can be obtained on plastic substrates by a fast and flexible UV curing process, that can also be utilized for patterning. Such ITO nanocomposites therefore have to be considered a serious alternative to vacuum deposition or wet deposited organic metals in the deposition of transparent conducting coatings on plastics.

[1]   H. L. Hartnagel, A. L. Dawar, A. K. Jain, C. Jagadish, *Semiconducting Transparent Thin Films*, Institute of Physics Publishing, Bristol, **1995**.

[2]   H. J. Gläser, *Large area glass coating*, Von Ardenne Anlagentechnik, Dresden, **2000**.

[3]   F. Milde, J. Brückner, C. Deus, M. Kammer, H. Neumann in: *Proc. 4th Int. Conf. on Coatings on Glass, ICCG*, **2002**, p. 419–424.

[4]   S. F. Kistler, P. M. Schweizer (Eds.), *Liquid Film Coating*, Chapman & Hall, London, **1997**, Ch. 11.

[5]   J. Puetz, M. A. Aegerter, in: *Handbook on Sol-Gel Technologies for Glass Producers and Users*, Kluwer Academic Publishers (Norwell) (**2004**). accepted.

[6]   R. Nonninger, C. Goebbert, H. Schmidt, R. Drumm, S. Sepeur, *US Patent 6.533.966*, **1999**.

[7]   D. Burgard, C. Kropf, R. Nass, H. Schmidt, *MRS Symp. Proc.* **1994**, Vol. 346, p. 101–107.

[8]   B. Wessling, *Synth. Metals* **2003**, *153*, 265.

[9]   B. L. Groenendaal, F. Jonas, D. Freitag, H. Pielartzik, J. R. Reynolds, *Adv. Mater.* **2000**, *12*, 481.

[10] N. Al-Dahoudi, *PhD Thesis*, INM and University of Saarland, Shaker Verlag, Aachen, **2003**.

[11] H. K. Schmidt, *Macromol. Symp.* **1996**, *101*, p. 333–342.

[12] M. A. Aegerter, N. Al-Dahoudi, A. Solieman, H. Kavak, P. Oliveira in: *Proc. 7th ICFPAM, June 10–15*, **2003**, Bucharest, Romania.